Mouse models of non-dystrophic and dystrophic myotonia exhibit nociplastic pain-like behaviors

Tyler S. Nelson[1], Paz Duran[2], Aida Calderon-Rivera[1], Kimberly Gomez[1], Santiago Loya-Lopez[1], Rajesh Khanna[1*]

1. Department of Pharmacology and Therapeutics, McKnight Brain Institute, and Pain and Addiction Therapeutics (PATH) Collaboratory, University of Florida College of Medicine, Gainesville, FL 32610, USA
2. Department of Molecular Pathobiology, College of Dentistry, New York University, New York, NY 10010, USA

***Corresponding author**:
Name: Rajesh Khanna, Ph.D.
Mailing Address: 1149 Newell Drive, Room, Gainesville, FL 32610, USA
Email: r.khanna@ufl.edu

Conflicts of Interest: R.K. is the founder of Regulonix LLC, a company developing non-opioids drugs for chronic pain.

Abstract

Pain is a prominent and debilitating symptom in myotonic disorders, yet its physiological mechanisms remain poorly understood. This study assessed preclinical pain-like behavior in murine models of pharmacologically induced myotonia and myotonic dystrophy type 1 (DM1). In both myotonia congenita and DM1, impairment of the *CLCN1* gene, which encodes skeletal muscle voltage-gated CLC-1 chloride channels, reduces chloride ion conductance in skeletal muscle cells, leading to prolonged muscle excitability and delayed relaxation after contraction. We used the CLC-1 antagonist anthracene-9-carboxylic acid (9-AC) at intraperitoneal doses of 30 or 60 mg/kg and HSA LR20b DM1 mice to model CLC-1-induced myotonia. Our experimental approach included *in vivo* pain behavioral testing, *ex vivo* calcium imaging, and whole-cell current-clamp electrophysiology in mouse dorsal root ganglion (DRG) neurons. A single injection of 9-AC induced myotonia in mice, which persisted for several hours and resulted in long-lasting allodynic pain-like behavior. Similarly, HSA LR20b mice exhibited both allodynia and hyperalgesia. Despite these pain-like behaviors, DRG neurons did not show signs of hyperexcitability in either myotonic model. These findings suggest that myotonia induces nociplastic pain-like behavior in preclinical rodents, likely through central sensitization mechanisms rather than peripheral sensitization. This study provides insights into the pathophysiology of pain in myotonic disorders and highlights the potential of using myotonic mouse models to explore pain mechanisms and assess novel analgesics. Future research should focus on the central mechanisms involved in myotonia-induced pain and develop targeted therapies to alleviate this significant clinical burden.

Introduction

Myotonic disorders encompass a range of neuromuscular conditions characterized by persistent muscle contractions and impaired relaxation (Heatwole *et al.*, 2013; Trivedi, 2022). Myotonia, a hallmark feature, arises from heightened electrical excitability in muscles, primarily due to mutations in the genes *SCN4A* and *CLCN1*, which encode the skeletal muscle voltage-gated Nav1.4 sodium and CLC-1 chloride channels, respectively (Stunnenberg *et al.*, 2020). Clinical manifestations of myotonia vary, from obvious delays in muscle relaxation to subtle findings detectable through electromyography (EMG) (Miller, 2008; Matthews *et al.*, 2010; Stunnenberg *et al.*, 2020). Myotonia often leads to severe muscle stiffness, impaired movement, and debilitating pain, increasing the risk of falls and reducing quality of life (Sansone *et al.*, 2012; Trivedi *et al.*, 2013; Matthews *et al.*, 2021).

CLCN1 plays a crucial role in regulating skeletal muscle excitability and contraction by facilitating chloride ion flux across the muscle membrane (Pedersen *et al.*, 2016). Dysfunction of *CLCN1* results in impaired chloride ion transport, leading to prolonged depolarization and delayed muscle relaxation (Tang & Chen, 2011). For instance, mutations affecting *CLCN1* produce both autosomal dominant (Thomsen's disease) and autosomal recessive (Becker's disease) myotonia congenita, hereditary neuromuscular disorders characterized by muscle stiffness and delayed relaxation (Steinmeyer *et al.*, 1991; Koch *et al.*, 1992; Zhang *et al.*, 1996; Plassart-Schiess *et al.*, 1998). Similarly, in myotonic dystrophy type 1 (DM1), abnormal splicing of *CLCN1* reduces the expression of the CLC-1 chloride channel in skeletal muscle cells, contributing to muscle hyperexcitability and the characteristic myotonia observed in this condition (Charlet-B *et al.*, 2002; Mankodi *et al.*, 2002; Lueck *et al.*, 2007).

Nearly 100 years of pre-clinical research demonstrates that monocarboxylic aromatic acids elicit myotonic symptoms in mammalian and amphibious skeletal muscle tissue (Pohl & Hesse, 1925; Eddy, 1933; Smith, 1935; Bryant & Morales-Aguilera, 1971; Brody, 1973; Palade & Barchi, 1977; Furman & Barchi, 1978; Bretag *et al.*, 1980; Kwieciński & Barchi, 1981). These compounds produce sudden muscle stiffness and repetitive firing and 'dive-bomber' patterns that are detectable with extracellular or intracellular electromyography (Smith, 1935; Furman & Barchi, 1978). Anthracene-9-carboxylic acid (9-AC) is one of the most well characterized monocarboxylic aromatic acids and produces myotonia in rodent (Mrozek *et al.*, 1974; Camerino *et al.*, 1989; Desaphy *et al.*, 2013, 2014), rabbit (Villegas-Navarro *et al.*, 1986), goat (Bryant & Morales-Aguilera, 1971), canine (Welsh, 1984), porcine (Bandschapp *et al.*, 2009), and human skeletal muscle (Kwiecińaski *et al.*, 1988). 9-AC produces rapid myotonic symptoms following systemic delivery via specifically blocking the skeletal muscle-type chloride channel ClC-1 (Bryant & Morales-Aguilera, 1971; Villegas-Navarro *et al.*, 1986; Estévez *et al.*, 2003; Altamura *et al.*, 2018). Thus, *in vivo* assessment of the efficacy of anti-myotonic drugs and muscle relaxants has been routinely employed in rodents following 9-AC administration (Sethi, 1976; Desaphy *et al.*, 2013, 2014, 2020; De Bellis *et al.*, 2017).

However, to our knowledge no study to date has evaluated 9-AC-induced myotonia and its effect on pain-like behavior. Although episodic weakness, myotonia, and muscular manifestations are the most described clinical symptoms in myotonic disorders, pain emerges as a frequently reported symptom and is often the patient's main concern (Trip *et al.*, 2009; Sansone *et al.*, 2012; Meyer *et al.*, 2020; Giacobbe *et al.*, 2021). For example, high impact pain that affects quality of life is reported in patients afflicted with myotonia congenita (Sanders, 1976; Sunohara *et al.*, 1996; Trivedi *et al.*, 2013; Nam *et al.*, 2015; Orsini *et al.*, 2020), myotonic dystrophies (Jensen *et al.*, 2008; Miró *et al.*, 2014; Parmova, 2014; Peric *et al.*, 2015; Moshourab *et al.*, 2016; van Vliet *et al.*, 2018; Solbakken *et al.*, 2021; Liguori *et al.*, 2023), and *SCN4A*-related myotonic disorders (Bissay *et al.*, 2011; Torbergsen *et al.*, 2015; Palmio *et al.*, 2017; Suokas *et al.*, 2018; Giacobbe *et al.*, 2021). However, the underlying mechanisms linking myotonia to pain remain poorly understood. Due to the high prevalence of pain in inherited myotonic disorders (Meyer *et al.*, 2020), we hypothesized that 9-AC administration may produce pain-like behavior in rodents. Our results unveil that a single myotonic episode elicits symptoms consistent with nociplastic pain, thus highlighting a causal relationship between myotonia and chronic pain development.

Methods

Animals

Adult C57Bl/6J (Jackson Laboratory, # 000664), FVB/NJ (Jackson Laboratory, # 001800) and (FVB/N-Tg(HSA*LR)20bCath/J (Jackson Laboratory #032031) male and female mice were group housed, provided access to food and water *ad libitum*, and maintained on a 12:12 hour light:dark cycle in temperature and humidity controlled rooms. Equal numbers of male and female mice were used in all experiments. Although we were not powered to detect significant sex differences, no major/obvious trends in sex differences were observed and means from both sexes were pooled. All procedures were consistent with the guidelines for the treatment of animals of the International Association for the Study of Pain and were approved by New York University's Institutional Animal Care and Use Committee.

Drug Administration

Anthracene-9-carboxylic acid, 99% purity (Thermo Scientific, # 104880100), was diluted in a solution containing 50% dimethyl sulfoxide and 50% sterile 0.9% sodium chloride, while the vehicle comprised the same constituents. The drug was freshly prepared each day just before administration due to its tendency to precipitate out of solution rapidly. Mice were briefly scruffed and received a single intraperitoneal (i.p.) injection using a 30-gauge needle.

Calcium Imaging

Changes in calcium influx in mouse DRG neurons were determined as previously described (Moutal *et al.*, 2016; Duran *et al.*, 2022). DRG neurons were dissected and cultured 24 hours after 9-AC administration (60 mg/kg, i.p.) as previously described (Gomez *et al.*, 2023*b*, 2024). DRG neurons were loaded for 30 min at 37°C with 3 μM of Fura-2AM (Cat. No. F1221, Thermo Fisher Scientific, stock solution prepared at 1 mM in DMSO with 0.02% pluronic acid, Cat. No. P-3000MP, Life Technologies) to see changes in intracellular calcium $[Ca^{2+}]c$ in a standard Tyrode's bath solution containing 139 mM NaCl, 3 mM potassium chloride (KCl), 0.8 mM $MgCl_2$, 1.8 mM $CaCl_2$, 5 mM glucose and 10 mM Na HEPES (pH 7.4). Cells were first examined under bright field to exclude those showing signs of lysis. To determine the changes in ligand-induced calcium influx, baseline was acquired for 1 minute, then Ca^{2+} influx was stimulated with a 15 s pulse with 200 nM capsaicin or 400 nM menthol diluted in the standard Tyrode's solution. Response was followed for 6 min while bath solution was continuously perfused over the cells to wash off excess of the trigger. This process was automated using the software WinTask ×64 (Version 5.1, WinTask) that controlled the perfusion of the standard bath solution and triggers through Valvelink 8.2 software (Automate Scientific). At the end of the protocol, cell viability was assessed by depolarization-induced Ca^{2+} influx using and an excitatory 90 mM KCl solution. Fluorescence imaging was performed with an inverted microscope, Nikon Eclipse TE2000-U (New York, NY, USA), using objective Nikon Super Fluor 20 × 0.75 NA and a Photometrics cooled CCD camera CoolSNAPHQ (Roper Scientific, Tucson, AZ, USA) controlled by MetaFluor 6.3 software (Molecular Devices, Downingtown, PA, USA). The excitation

light was delivered by a Lambda-LS system (Sutter Instrument, Novato, CA, USA). The excitation filters (340 ± 5 and 380 ± 7) were controlled by a Lambda 10-2 optical filter change (Sutter Instrument). Fluorescence was recorded through a 505 nm dichroic mirror at 535 ± 25 nm. To minimize phototoxicity and photobleaching, the images were taken every ~10 s during the time course of the experiment using the minimal exposure time that provided acceptable image quality. Changes in $[Ca^{2+}]c$ were monitored by following a ratio of F340/F380, calculated after the subtraction of the background from both channels.

Electrophysiological recordings in sensory neurons

Dorsal root ganglion neuron cultures were performed as previously described (Gomez *et al.*, 2023*b*, 2024). Briefly, lumbar DRG neurons were dissected from 3 months old male and female mice. The tissue was dissociated enzymatically in DMEM media containing collagenase type I (1.66 mg/mL, Cat# LS004194; Worthington) and neutral protease (1.04 mg/mL, Cat# LS02104; Worthington, Lakewood, NJ) for 50 minutes at 37°C with gentle see-saw motion. The dissociated cells were collected by centrifugation (800 rpm, 5 min) and plated on 12-mm coverslips pre-coated with poly-D-lysine (0.1 mg/ml, Cat# P6407, Millipore Sigma, St. Louis, MO). The culture media was supplemented with 10% fetal bovine serum (HyClone) and 1% penicillin/streptomycin sulfate (Cat# 15140, Life Technologies, Carlsbad, CA). The neuronal excitability was assessed 15–24 h after plating the neurons.Whole-cell current-clamp recordings. Acutely dissociated DRG neurons were subjected to whole-cell patch-clamp technique and current clamp mode, as previously described (Finol-Urdaneta *et al.*, 2022). Recordings were conducted at room temperature (20–22°C) using an EPC 10 Amplifier-HEKA (HEKA Elektronik, Ludwigshafen, Germany) and Patchmaster software. Briefly, electrical giga-seals were formed between the cell membrane and borosilicate glass electrodes. Negative pressure was applied to establish the whole cell configuration, then voltage clamp mode was changed to current clamp. The electrical resistance of electrodes was ~2–3.5 MΩ when filled with the internal solution (see solutions). Action potentials were evoked by a ramp pulse from 0-150 pA in 1 sec, the ramp was applied thrice, and the average of each neuron was plotted. Rheobase was measured by injecting current from 0 pA in increments of 10 pA. Composition of the external solution (in mM): 140 NaCl, 4 KCl, 2 $CaCl_2$, $MgCl_2$, 10 HEPES, 10 Glucose. Internal solution (in mM): 120 K-gluconate, 10 NaCl, 4 Mg-ATP, 10 HEPES, 5 EGTA, 2 $MgCl_2$.

Behavioral Testing

Static Mechanical Sensitivity (von Frey): Testing was performed as previously described(Nelson *et al.*, 2022, 2023; Gomez *et al.*, 2023*a*). Mice were habituated to plexiglass chambers (80 × 80 × 110 mm) on a raised wire mesh platform for 60 minutes immediately prior to behavioral testing. Testing was performed using a calibrated set of logarithmically increasing von Frey monofilaments (Braintree Scientific Cat: 58011) that range in gram force from 0.007 to 6.0 g. Beginning with a 0.4 g filament, these were applied perpendicular to the lateral hindpaw surface with sufficient force to cause a slight bending of the filament. A positive response was denoted as a rapid withdrawal of the paw within 4 seconds of application and

was followed by application of the next lower filament. A negative response was followed by application of the next higher filament. An up-down method (Chaplan *et al.*, 1994) was used to calculate the 50% withdrawal threshold for each mouse.

Dynamic Mechanical Sensitivity (Brush): Immediately following von Frey testing, dynamic mechanical sensitivity testing was performed on mice in the same plexiglass chambers on a raised wire mesh platform. A cotton swab was “puffed-out” to about three times its original size. The left hindpaw was then brushed using this cotton swab in the heel-to-toe direction. A positive response was noted as a rapid withdrawal of the paw in response to stimulation. The test was repeated four times, and the frequency of responses was reported.

Cool Withdrawal Duration (Acetone): Testing was performed as previously described (Nelson *et al.*, 2022, 2023; Gomez *et al.*, 2023*a*). Immediately following dynamic brush testing, sensitivity to non-noxious cold testing was performed on mice in the same plexiglass chambers on a raised wire mesh platform. Using a syringe connected to PE-90 tubing, flared at the tip to a diameter of 3 1/2 mm, we applied a drop of acetone (VWR Cat: BDH1101-1LP) to the plantar surface of the hind left paw. Surface tension maintained the volume of the drop to ~10 μL. The duration of time the animal lifted or shook its paw was recorded for 30 s. Three observations were averaged.

Time to Righting Reflex (TRR): Mice were gently placed on their backs on a flat surface to initiate the test. The duration it took for the mouse to return to an upright position, termed the righting reflex, was recorded. Each trial was repeated three times at each time point, and the average of these observations was calculated. This reflex serves as an indicator of the mouse's motor coordination and recovery capability. In healthy mice, the typical time to right itself is less than 0.5 seconds.

Thermal Withdrawal Threshold (Hot/Cold Plate): We evaluated acute nociceptive responses with a hot plate as previously described (Nelson *et al.*, 2019, 2022; Qi *et al.*, 2023). Briefly, prior to testing mice acclimated to the testing room for at least 30 minutes to minimize stress-induced behaviors. Following acclimation, mice were gently placed on a 0-55 °C Ugo Basile hot/cold plate (Stoelting Cat:55075). The trial ended when the mouse exhibited a nociceptive response (such as paw licking or jumping) or after a cutoff time of 30 seconds if no response was observed. Testing was repeated for 3 trials per mouse per temperature with intervals of at least 10 minutes between each trial. The latency to respond for each trial was averaged to produce the mean latency for statistical analysis.

Results

Anthracene-9-carboxylic acid (9-AC) produces *in vivo* myotonic and chronic pain-like behavior in mice.

First, we confirmed that intraperitoneal (i.p.) injection of 9-AC at doses ranging from 30 to 60 mg/kg induced myotonia in mice. Consistent with previous reports in both mice (Sethi, 1976) and rats (Mrozek *et al.*, 1974; Desaphy *et al.*, 2013), within minutes of a single dose of 9-AC, mice exhibited evident gait abnormalities, cramping, muscle stiffness, and motor difficulties. Importantly, there were no discernible alterations in respiration or consciousness. Myotonia was assessed by measuring the time of righting reflex (TRR), as described previously (Desaphy *et al.*, 2013, 2014) (**Figure 1A**). We observed a dose-dependent increase in TRR lasting up to 180 minutes post-9-AC administration. (**Figure 1B-C**).

Next, we investigated the impact of a single dose of 9-AC on producing behavioral signs of pain. At the 24-hour mark post-9-AC administration, a time when myotonia had resolved, we assessed behavioral indicators of mechanical and thermal allodynia and hyperalgesia (**Figure 2A**). Notably, 9-AC but not vehicle administration reduced the mechanical withdrawal threshold of mice (**Figure 2B**), heightened responsiveness to light brushing of the hindpaw (**Figure 2C**), and increased flinching behavior in response to acetone application to the hindpaw (**Figure 2D**). These symptoms are indicative of static and dynamic mechanical allodynia as well as cold allodynia. However, 9-AC did not induce thermal hyperalgesia in response to either noxious cold or noxious heat stimuli (**Figure 2E**). Overall, these findings suggest that a single episode of 9-AC-induced myotonia resulted in prolonged mechanical and cold allodynia, but not hyperalgesia.

Anthracene-9-carboxylic acid does not increase the excitability of sensory neurons.

Next, we investigated the underlying pathophysiological mechanisms driving 9-AC induced pain-like behavior. Pain is often triggered by peripheral and/or central sensitization of nociceptive pathways (Gold & Gebhart, 2010; Kuner, 2010). We hypothesized that 9-AC-induced myotonia produced pain-like behavior via peripheral sensitization/increasing the excitability of dorsal root ganglion (DRG) primary sensory neurons. To test this hypothesis, we first evaluated the excitability of DRG neurons in mice 24 hours post-9-AC (60 mg/kg, i.p.) or vehicle treatment using *ex vivo* calcium imaging. We subjected DRGs of all sizes to three distinct challenges: KCl (90 mM) to evaluate the activity of high-voltage-activated Ca^{2+} channels, capsaicin (200 nM) to gauge the activity of the heat receptor transient receptor potential vanilloid 1 (TRPV1) channels, and menthol (400 nM) to assess the activity of the cold receptor transient receptor potential cation channel subfamily melastatin member 8 (TRPM8) (**Figure 3A**). Reliably, all three stimuli produced calcium responses in sensory neurons (**Figure 3B**), however, we found no changes in average response to any stimuli in 9-AC-treated mice in comparison to vehicle treated mice (**Figure 3C-E**).

In addition to calcium imaging, we also used *ex vivo* electrophysiology to evaluate the excitability of sensory neurons. The excitability was measured by injecting a ramp of current from 0-150 pA into the soma of small- and medium-diameter DRG neurons to elicit action potentials (Aps). We found that 9-AC did not affect the resting membrane potential (**Figure 4A**), the rheobase (**Figure 4B**), nor the number of Aps produced by current injection (**Figure 4C**). Together, these results indicate that a single administration of 9-AC (60 mg/kg, i.p.) does not increase the excitability of DRG primary sensory neurons.

<u>A mouse model of myotonic dystrophy type 1 exhibits a chronic pain-like phenotype.</u>

A single dose of 9-AC induces a myotonic episode similar to that seen in myotonia congenita (Bryant & Morales-Aguilera, 1971) and causes pain-like behavior (**Figure 2**). However, most patients do not experience just a single isolated myotonic episode. Instead, genetic mutations result in recurrent myotonic episodes throughout life. Therefore, we hypothesized that mice with myotonia-producing genetic mutations may exhibit persistent pain-like behavior. To test this hypothesis, we used the well characterized HSA LR20b transgenic mouse model of DM1. This genetically engineered mouse model carries a transgene for human skeletal actin (HSA) with an expanded CTG repeat sequence of ~220 repeats in the 3' untranslated region, mimicking the CTG repeat expansion in the *DMPK* gene seen in human DM1 (Mankodi *et al.*, 2000). The expression of expanded CTG repeats triggers aberrant splicing of *Clcn1* in skeletal muscle and reduces the surface expression of CLC-1 in muscle fibers producing recurrent myotonia in these mice (Charlet-B *et al.*, 2002; Mankodi *et al.*, 2002). As hypothesized, we found that adult HSA LR20b mice exhibited both static (**Figure 5A**) and dynamic mechanical allodynia (**Figure 5B**), cold allodynia (**Figure 5C**), and heat hyperalgesia (**Figure 5D**) in comparison to wildtype background strain mice.

Lastly, we again utilized calcium imaging to evaluate the excitability of DRG neurons from wildtype or DM1 mice. We again challenged DRGs of all sizes to KCl (90 mM), capsaicin (200 nM), and menthol (400 nM) (**Figure 6A**). Reliably, all three stimuli produced calcium responses in sensory neurons (**Figure 6B**), however, we found no changes in average response to any stimuli in DM1 mice in comparison to WT mice (**Figure 6C-E**). These results suggest that DM1 mice exhibit persistent allodynic and hyperalgesic pain behavior but do not exhibit evidence of excitability of DRG primary sensory neurons.

Discussion

In this paper, we present evidence for the first time that preclinical models of myotonia exhibit pain-like behavior. Additionally, we provide physiological data suggesting that this pain-like behavior is not driven by hyperexcitability of peripheral sensory neurons (i.e., peripheral sensitization).

Patients with both dystrophic and non-dystrophic myotonic disorders experience generalized muscle cramping and myalgia (Jensen *et al.*, 2008; Peric *et al.*, 2015; Giacobbe *et al.*, 2021). Interestingly, *CLCN1*, the gene responsible for chloride imbalance and myotonia in muscles, is predominately expressed in muscle tissue and not present in dorsal root ganglia (DRGs) before or after injury (Renthal *et al.*, 2020). Therefore, we hypothesized that rather than CLC-1 channels directly affecting nociceptor function, instead the repeated contraction/hyperexcitability of the muscle fiber sarcolemma (myotonia due to the *CLCN1* dysregulation) produces repetitive activation of nociceptive DRG free nerve endings that terminate in the muscles. This repeated activation of nociceptive free endings may drive plasticity in nociceptive DRG and/or dorsal horn/brain neurons (peripheral and/or central sensitization), reducing the threshold for a pain-like response and amplifying the responsiveness to sensory stimulation (Latremoliere & Woolf, 2009; Gangadharan & Kuner, 2013). However, our *ex vivo* electrophysiology and calcium imaging data suggest that peripheral sensitization is likely not responsible for the pain-like behavior. While rigorous quantitative sensory testing in myotonic patients has remained limited, our preclinical data aligns with multiple studies that have demonstrated limited peripheral sensory neuron abnormalities in myotonic dystrophy patients (Hermans *et al.*, 2011; Peric *et al.*, 2013; Nojszewska *et al.*, 2015; Boland-Freitas & Ng, 2019). Nevertheless, we cannot rule out peripheral involvement as an initial priming event for central sensitization. Future studies should test the hypothesis that myotonia produces nociplastic pain behavior via central sensitization of neural pain circuits, such as the spinal and/or parabrachial nucleus neural populations (Nelson & Allen, 2023; Condon *et al.*, 2024).

Recently, an international community of pain researchers described a third category of pain, termed “nociplastic pain,” which is mechanistically distinct from nociceptive pain (produced by ongoing inflammation or tissue damage) and neuropathic pain (produced by a lesion or damage to the somatosensory system) (Kosek *et al.*, 2016). Nociplastic pain presents as multifocal pain without discernable tissue or nerve damage, alongside central nervous system comorbidities such as fatigue, sleep disturbances, and mood disorders. Although the mechanisms of nociplastic pain are not completely understood, it is thought that augmented central sensitization and pain modulation are key contributors (Fitzcharles *et al.*, 2021; Kaplan *et al.*, 2024). Among the three types of pain, myotonia-induced pain best represents a form of nociplastic pain or pain phenotype that arises from altered nociception in the absence of tissue damage. Supporting this idea, myotonic disorders and fibromyalgia syndrome (FMS) appear phenotypically similar, as both involve diffuse chronic widespread muscle pain and significant comorbidities (Nam *et al.*, 2015). Due to these overlapping symptoms, myotonic disorders are often

misdiagnosed as FMS or meet the FMS diagnosis criterion (Götze *et al.*, 1998; Auvinen *et al.*, 2008; Nam *et al.*, 2015; Giacobbe *et al.*, 2021). Future preclinical and clinical studies should continue to investigate central mechanisms of nociplastic pain in myotonic disorders.

To the best of our knowledge, this is the first study to evaluate pain-like pathophysiology in a preclinical model of myotonia. The evidence of pain in these mouse models presents a new opportunity for researchers to evaluate both pain-driving pathophysiological mechanisms and screen new analgesics. Currently there are limited to no pain treatment options for myotonic disorders or other nociplastic pain disorders. Myotonic disorders are rare in the human population, making it difficult to perform rigorous quantitative sensory testing studies to determine pain origins or to conduct double-blinded placebo-controlled studies to evaluate the efficacy of novel analgesics. In contrast, mice breed quickly and present a fantastic model organism to rapidly investigate pain in myotonic disorders.

One limitation of this study is that we simplify the myotonic disorder experience to only CLC-1 blockade/ dysregulation. By contrast, myotonic patients, particularly those with myotonic dystrophies, often present with a range of neurological comorbidities and muscle pathologies that can significantly complicate their pain experience. Despite this complexity, our primary aim was to investigate whether a single myotonic episode or recurrent episodes could induce pain-like behavior and sensory neuron pathology. To achieve this, we used the CLC-1 preferring antagonist, 9-AC, and utilized a mouse model of DM1 that primarily mimics muscle pathology while overlooking CTG repeats in other body systems, including the nervous system. We consider this approach a strength of our study as it directly implicates myotonia as a causal factor for pain behavior, a connection not previously established. However, it's essential to acknowledge that future research may reveal differences in peripheral sensory involvement compared to what we observed here, especially when using alternative myotonic models or different experimental designs. For instance, our evaluation of pain-like behavior only after a single injection of 9-AC may overlook potential changes in DRG plasticity that could occur with repeated injections. Additionally, we did not delve into the relationship between muscle fiber pathology and pain-like behavior. Different sensory pathologies might correspond with specific muscle dysregulations or fiber types. Notably, another murine model of DM1 myotonia has shown transitions between glycolytic and oxidative fiber types (Hu *et al.*, 2023) and such a transition may affect pain pathophysiology. Finally, it's important to note that some patients experience painful myotonia due to *SCN4A* mutations rather than *CLCN1*, and this type of myotonia was not addressed in our preclinical study.

In conclusion, this study provides the first evidence that preclinical models of myotonia exhibit pain-like behavior, implicating myotonia as a direct cause of pain. Our findings indicate that this pain-like behavior is not driven by peripheral sensitization, suggesting central mechanisms might be involved. While we focused on CLC-1 dysregulation, future research should explore other genetic mutations and the

relationship between muscle pathology and pain. These results open new avenues for understanding pain mechanisms in myotonic disorders and developing effective treatments, addressing a significant unmet need in pain management for these conditions.

Acknowledgements

This work was supported was supported by National Institutes of Health (NIH) awards K00NS124190 (to TSN), and RF1NS131165, R61NS126026, R01NS120663 (to RK). Additionally, this work was supported by a Development Grant from the American Neuromuscular Foundation (to TSN).

References

Altamura C, Mangiatordi GF, Nicolotti O, Sahbani D, Farinato A, Leonetti F, Carratù MR, Conte D, Desaphy JF & Imbrici P (2018). Mapping ligand binding pockets in chloride ClC-1 channels through an integrated in silico and experimental approach using anthracene-9-carboxylic acid and niflumic acid. *Br J Pharmacol* **175,** 1770–1780.

Auvinen S, Suominen T, Hannonen P, Bachinski LL, Krahe R & Udd B (2008). Myotonic dystrophy type 2 found in two of sixty-three persons diagnosed as having fibromyalgia. *Arthritis Rheum* **58,** 3627–3631.

Bandschapp O, Ginz HF, Soule CL, Girard T, Urwyler A & Iaizzo PA (2009). In Vitro Effects of Propofol and Volatile Agents on Pharmacologically Induced Chloride Channel Myotonia. *Anesthesiology* **111,** 584–590.

De Bellis M, Carbonara R, Roussel J, Farinato A, Massari A, Pierno S, Muraglia M, Corbo F, Franchini C, Carratù MR, De Luca A, Conte Camerino D & Desaphy J-F (2017). Increased sodium channel use-dependent inhibition by a new potent analogue of tocainide greatly enhances in vivo antimyotonic activity. *Neuropharmacology* **113,** 206–216.

Bissay V, Keymolen K, Lissens W, Laureys G, Schmedding E & Keyser J De (2011). Late onset painful cold-aggravated myotonia: Three families with SCN4A L1436P mutation. *Neuromuscul Disord* **21,** 590–593.

Boland-Freitas R & Ng K (2019). Assessment of small sensory fiber function in myotonic dystrophy type 1. *Muscle and Nerve* **60,** 575–579.

Bretag AH, Dawe SR & Moskwa AG (1980). Chemically induced myotonia in amphibia. *Nature* **286,** 625–626.

Brody IA (1973). Myotonia Induced by Monocarboxylic Aromatic Acids. *Arch Neurol* **28,** 243.

Bryant SH & Morales-Aguilera A (1971). Chloride conductance in normal and myotonic muscle fibres and the action of monocarboxylic aromatic acids. *J Physiol* **219,** 367–383.

Camerino DC, De Luca A, Mambrini M, Ferrannini E, Franconi F, Giotti A & Bryant SH (1989). The effects of taurine on pharmacologically induced myotonia. *Muscle Nerve* **12,** 898–904.

Chaplan SR, Bach FW, Pogrel JW, Chung JM & Yaksh TL (1994). Quantitative assessment of tactile allodynia in the rat paw. *J Neurosci Methods* **53,** 55–63.

Charlet-B N, Savkur RS, Singh G, Philips A V, Grice EA & Cooper TA (2002). Loss of the Muscle-Specific Chloride Channel in Type 1 Myotonic Dystrophy Due to Misregulated Alternative Splicing several lines of evidence indicate that a gain of function for RNA CUG)n. *Mol Cell* **10,** 45–53.

Condon LF, Yu Y, Park S, Cao F, Pauli JL, Nelson TS & Palmiter RD (2024). Parabrachial Calca neurons drive nociplasticity. *Cell Rep* **43,** 114057.

Desaphy JF, Carbonara R, Costanza T & Conte Camerino D (2014). Preclinical evaluation of marketed sodium channel blockers in a rat model of myotonia discloses promising antimyotonic drugs. *Exp*

Neurol **255,** 96–102.

Desaphy JF, Costanza T, Carbonara R & Conte Camerino D (2013). In vivo evaluation of antimyotonic efficacy of β-adrenergic drugs in a rat model of myotonia. *Neuropharmacology* **65,** 21–27.

Desaphy JF, Farinato A, Altamura C, De Bellis M, Imbrici P, Tarantino N, Caccia C, Melloni E, Padoani G, Vailati S, Keywood C, Carratù MR, De Luca A, Conte D & Pierno S (2020). Safinamide's potential in treating nondystrophic myotonias: Inhibition of skeletal muscle voltage-gated sodium channels and skeletal muscle hyperexcitability in vitro and in vivo. *Exp Neurol* **328,** 113287.

Duran P et al. (2022). The natural product Argentatin C attenuates postoperative pain via inhibition of voltage-gated sodium and T-type voltage-gated calcium channels. *Br J Pharmacol*1–19.

Eddy NB (1933). Studies of Phenanthrene Derivatives I. A Comparison of Phenanthrene 2-, 3-, and 9-Monosubstitution Products. *J Pharmacol Exp Ther* **48,** 183–198.

Estévez R, Schroeder BC, Accardi A, Jentsch TJ & Pusch M (2003). Conservation of chloride channel structure revealed by an inhibitor binding site in ClC-1. *Neuron* **38,** 47–59.

Finol-Urdaneta RK et al. (2022). Multitarget nociceptor sensitization by a promiscuous peptide from the venom of the King Baboon spider. *Proc Natl Acad Sci* **119,** 1–12.

Fitzcharles MA, Cohen SP, Clauw DJ, Littlejohn G, Usui C & Häuser W (2021). Nociplastic pain: towards an understanding of prevalent pain conditions. *Lancet* **397,** 2098–2110.

Furman RE & Barchi RL (1978). The pathophysiology of myotonia produced by aromatic carboxylic acids. *Ann Neurol* **4,** 357–365.

Gangadharan V & Kuner R (2013). Pain hypersensitivity mechanisms at a glance. *DMM Dis Model Mech* **6,** 889–895.

Giacobbe A, Subramony S & Chuquilin M (2021). Pain as a significant symptom in patients with periodic paralysis—A cross-sectional survey. *Muscle and Nerve* **63,** 897–901.

Gold MS & Gebhart GF (2010). Nociceptor sensitization in pain pathogenesis. *Nat Med* **16,** 1248–1257.

Gomez K et al. (2023*a*). A peptidomimetic modulator of the CaV2.2 N-type calcium channel for chronic pain. *Proc Natl Acad Sci* **120,** e2305215120.

Gomez K, Allen HN, Duran P, Loya-Lopez S, Calderon-Rivera A, Moutal A, Tang C, Nelson TS, Perez-Miller S & Khanna R (2024). Targeted transcriptional upregulation of SENP1 by CRISPR activation enhances deSUMOylation pathways to elicit antinociception in the spinal nerve ligation model of neuropathic pain. *Pain* **165,** 866–883.

Gomez K, Duran P, Tonello R, Allen HN, Boinon L, Calderon-Rivera A, Loya-López S, Nelson TS, Ran D, Moutal A, Bunnett NW & Khanna R (2023*b*). Neuropilin-1 is essential for vascular endothelial growth factor A–mediated increase of sensory neuron activity and development of pain-like behaviors. *Pain* **164,** 2696–2710.

Götze FR, Thid S & Kyllerman M (1998). Fibromyalgia in hyperkalemic periodic paralysis. *Scand J Rheumatol* **27,** 383–384.

Heatwole CR, Statland JM & Logigian EL (2013). The diagnosis and treatment of myotonic disorders.

Muscle Nerve **47,** 632–648.

Hermans MCE, Faber CG, Vanhoutte EK, Bakkers M, De Baets MH, De Die-Smulders CEM & Merkies ISJ (2011). Peripheral neuropathy in myotonic dystrophy type 1. *J Peripher Nerv Syst* **16,** 24–29.

Hu N, Kim E, Antoury L & Wheeler TM (2023). Correction of Clcn1 alternative splicing reverses muscle fiber type transition in mice with myotonic dystrophy. *Nat Commun*; DOI: 10.1038/s41467-023-37619-1.

Jensen MP, Hoffman AJ, Stoelb BL, Abresch RT, Carter GT & McDonald CM (2008). Chronic Pain in Persons With Myotonic Dystrophy and Facioscapulohumeral Dystrophy. *Arch Phys Med Rehabil* **89,** 320–328.

Kaplan CM, Kelleher E, Irani A, Schrepf A, Clauw DJ & Harte SE (2024). Deciphering nociplastic pain: clinical features, risk factors and potential mechanisms. *Nat Rev Neurol*; DOI: 10.1038/s41582-024-00966-8.

Koch MC, Steinmeyer K, Lorenz C, Ricker K, Wolf F, Otto M, Zoll B, Lehmann-Horn F, Grzeschik K-H & Jentsch TJ (1992). The Skeletal Muscle Chloride Channel in Dominant and Recessive Human Myotonia. *Science (80-)* **257,** 797–800.

Kosek E, Cohen M, Baron R, Gebhart GF, Mico JA, Rice ASC, Rief W & Sluka AK (2016). Do we need a third mechanistic descriptor for chronic pain states? *Pain* **157,** 1382–1386.

Kuner R (2010). Central mechanisms of pathological pain. *Nat Med* **16,** 1258–1266.

Kwiecińaski H, Lehmann-Horn F & Rüdel R (1988). Drug-induced myotonia in human intercostal muscle. *Muscle Nerve* **11,** 576–581.

Kwieciński H & Barchi RL (1981). Myotonia Induced by Chemical Agents. *CRC Crit Rev Toxicol* **8,** 279–310.

Latremoliere A & Woolf CJ (2009). Central Sensitization: A Generator of Pain Hypersensitivity by Central Neural Plasticity. *J Pain* **10,** 895–926.

Liguori S, Moretti A, Toro G, Paoletta M, Palomba A, Barra G, Gimigliano F & Iolascon G (2023). Pain and Motor Function in Myotonic Dystrophy Type 1: A Cross-Sectional Study. *Int J Environ Res Public Health* **20,** 1–11.

Lueck JD, Lungu C, Mankodi A, Osborne RJ, Welle SL, Dirksen RT & Thornton CA (2007). Chloride channelopathy in myotonic dystrophy resulting from loss of posttranscriptional regulation for CLCN1. *Am J Physiol - Cell Physiol* **292,** 1291–1297.

Mankodi A, Logigian E, Callahan L, McClain C, White R, Henderson D, Krym M & Thornton CA (2000). Myotonic dystrophy in transgenic mice expressing an expanded CUG repeat. *Science (80-)* **289,** 1769–1772.

Mankodi A, Takahashi MP, Jiang H, Beck CL, Bowers WJ, Moxley RT, Cannon SC & Thornton CA (2002). Expanded CUG repeats trigger aberrant splicing of ClC-1 chloride channel pre-mRNA and hyperexcitability of skeletal muscle in myotonic dystrophy. *Mol Cell* **10,** 35–44.

Matthews E, Fialho D, Tan S V., Venance SL, Cannon SC, Sternberg D, Fontaine B, Amato AA, Barohn

RJ, Griggs RC & Hanna MG (2010). The non-dystrophic myotonias: Molecular pathogenesis, diagnosis and treatment. *Brain* **133,** 9–22.

Matthews E, Holmes S & Fialho D (2021). Skeletal muscle channelopathies: A guide to diagnosis and management. *Pract Neurol* **21,** 196–205.

Meyer AP, Roggenbuck J, LoRusso S, Kissel J, Smith RM, Kline D & Arnold WD (2020). Genotype-Phenotype Correlations and Characterization of Medication Use in Inherited Myotonic Disorders. *Front Neurol* **11,** 593.

Miller TM (2008). Differential diagnosis of myotonic disorders. *Muscle Nerve* **37,** 293–299.

Miró J, Gertz KJ, Carter GT & Jensen MP (2014). Pain location and intensity impacts function in persons with myotonic dystrophy type 1 and facioscapulohumeral dystrophy with chronic pain. *Muscle and Nerve* **49,** 900–905.

Moshourab R, Palada V, Grunwald S, Grieben U, Lewin GR & Spuler S (2016). A Molecular Signature of Myalgia in Myotonic Dystrophy 2. *EBioMedicine* **7,** 205–211.

Moutal A, Chew LA, Yang X, Wang Y, Yeon SK, Telemi E, Meroueh S, Park KD, Shrinivasan R, Gilbraith KB, Qu C, Xie JY, Patwardhan A, Vanderah TW, Khanna M, Porreca F & Khanna R (2016). (S)-lacosamide inhibition of CRMP2 phosphorylation reduces postoperative and neuropathic pain behaviors through distinct classes of sensory neurons identified by constellation pharmacology. *Pain* **157,** 1448–1463.

Mrozek K, Kaminska A & Kwiecinski H (1974). Experimental myotonia myotonic activity of the fast and slow muscles. *Acta Physiol Pol* **25,** 321–327.

Nam TS, Choi SY, Park DJ, Lee SS, Kim YO & Kim MK (2015). The overlap between fibromyalgia syndrome and myotonia congenita. *J Clin Neurol* **11,** 188–191.

Nelson TS & Allen HN (2023). The spino-parabrachio-amygdaloid pathway is critical for the manifestation of chronic pain. *Neuropsychopharmacology*1–2.

Nelson TS, Fu W, Donahue RR, Corder GF, Hökfelt T, Wiley RG & Taylor BK (2019). Facilitation of neuropathic pain by the NPY Y1 receptor-expressing subpopulation of excitatory interneurons in the dorsal horn. *Sci Rep* **9,** 7248.

Nelson TS, Santos DFS, Prasoon P, Gralinski M, Allen HN & Taylor BK (2023). Endogenous μ-opioid—Neuropeptide Y Y1 receptor synergy silences chronic postoperative pain in mice. *PNAS Nexus* **2,** 1–11.

Nelson TS, Sinha GP, Santos DFS, Jukkola P, Prasoon P, Winter MK, McCarson KE, Smith BN & Taylor BK (2022). Spinal neuropeptide Y Y1 receptor-expressing neurons are a pharmacotherapeutic target for the alleviation of neuropathic pain. *Proc Natl Acad Sci U S A* **119,** e2204515119.

Nojszewska M, Łusakowska A, Szmidt-Salkowska E, Gaweł M, Lipowska M, Sułek A, Krysa W, Rajkiewicz M, Seroka A, Kaczmarek K & Kamińska AM (2015). Peripheral nerve involvement in myotonic dystrophy type 2 – similar or different than in myotonic dystrophy type 1? *Neurol Neurochir Pol* **49,** 164–170.

Orsini C, Petillo R, D'Ambrosio P, Ergoli M, Picillo E, Scutifero M, Passamano L, De Luca A & Politano L (2020). CLCN1 Molecular Characterization in 19 South-Italian Patients With Dominant and Recessive Type of Myotonia Congenita. *Front Neurol* **11,** 1–6.

Palade PT & Barchi RL (1977). On the inhibition of muscle membrane chloride conductance by aromatic carboxylic acids. *J Gen Physiol* **69,** 879–896.

Palmio J, Sandell S, Hanna MG, Männikkö R, Penttilä S & Udd B (2017). Predominantly myalgic phenotype caused by the c.3466G>A p.A1156T mutation in SCN4A gene. *Neurology* **88,** 1520–1527.

Parmova O (2014). The Character and Frequency of Muscular Pain in Myotonic Dystrophy and Their Relationship to Myotonia. *Int J Neurol Neurother* **1,** 1–5.

Pedersen TH, Riisager A, de Paoli FV, Chen TY & Nielsen OB (2016). Role of physiological ClC-1 Cl- ion channel regulation for the excitability and function of working skeletal muscle. *J Gen Physiol* **147,** 291–308.

Peric M, Peric S, Rapajic N, Dobricic V, Savic-Pavicevic D, Nesic I, Radojicic S, Novakovic I, Lavrnic D & Rakocevic-Stojanovic V (2015). Multidimensional aspects of pain in myotonic dystrophies. *Acta Myol myopathies cardiomyopathies Off J Mediterr Soc Myol* **34,** 126–132.

Peric S, Stojanovic VR, Nikolic A, Kacar A, Basta I, Pavlovic S & Lavrnic D (2013). Peripheral neuropathy in patients with myotonic dystrophy type 1. *Neurol Res* **35,** 331–335.

Plassart-Schiess E, Gervais A, Eymard B, Lagueny A, Pouget J, Warter JM, Fardeau M, Jentsch TJ & Fontaine B (1998). Novel muscle chloride channel (CLCN1) mutations in myotonia congenita with various modes of inheritance including incomplete dominance and penetrance. *Neurology* **50,** 1176–1179.

Pohl J & Hesse E (1925). Zur Pharmakologie des Tetrophans. *Klin Wochenschr* **4,** 343–344.

Qi Y, Nelson TS, Prasoon P, Norris C & Taylor BK (2023). Contribution of μ Opioid Receptor–expressing Dorsal Horn Interneurons to Neuropathic Pain–like Behavior in Mice. *Anesthesiology* **139,** 840–857.

Renthal W, Tochitsky I, Yang L, Cheng YC, Li E, Kawaguchi R, Geschwind DH & Woolf CJ (2020). Transcriptional Reprogramming of Distinct Peripheral Sensory Neuron Subtypes after Axonal Injury. *Neuron* **108,** 128-144.e9.

Sanders DB (1976). Myotonia Congenita With Painful Muscle Contractions. *Arch Neurol* **33,** 580–582.

Sansone VA, Ricci C, Montanari M, Apolone G, Rose M & Meola G (2012). Measuring quality of life impairment in skeletal muscle channelopathies. *Eur J Neurol* **19,** 1470–1476.

Sethi PD (1976). Antagonism of anthracene 9 carboxylic acid as screening test for muscle relaxants. *Indian J Physiol Pharmacol* **20,** 239–241.

Smith GR (1935). Studies of Phenanthrene Derivatives Iv. a Veratrine-Like Action on Skeletal Muscle of Certain 9-Substitution Products of Phenanthrene. *J Pharmacol Exp Ther* **54,** 87–99.

Solbakken G, Løseth S, Froholdt A, Eikeland TD, Nærland T, Frich JC, Dietrichs E & Ørstavik K (2021). Pain in adult myotonic dystrophy type 1: relation to function and gender. *BMC Neurol* **21,** 1–11.

Steinmeyer K, Klocke R, Ortland C, Gronemeier M, Jockusch H, GrÜnder S & Jentsch TJ (1991). Inactivation of muscle chloride channel by transposon insertion in myotonic mice. *Nature* **354,** 304–308.

Stunnenberg BC, LoRusso S, Arnold WD, Barohn RJ, Cannon SC, Fontaine B, Griggs RC, Hanna MG, Matthews E, Meola G, Sansone VA, Trivedi JR, van Engelen BGM, Vicart S & Statland JM (2020). Guidelines on clinical presentation and management of nondystrophic myotonias. *Muscle and Nerve* **62,** 430–444.

Sunohara N, Tomi H, Nakamura A, Arahata K & Nonaka I (1996). Myotonia congenita with painful muscle cramps. *Intern Med* **35,** 507–511.

Suokas K, Palmio J, Sandell S, Udd B & Hietaharju A (2018). Pain in SCN4A Mutated P.A1156T muscle sodium channelopathy—a postal survey. *Muscle and Nerve* **57,** 1014–1017.

Tang C-Y & Chen T-Y (2011). Physiology and Pathophysiology of CLC-1: Mechanisms of a Chloride Channel Disease, Myotonia. *J Biomed Biotechnol* **2011,** 1–10.

Torbergsen T, Jurkat-Rott K, Stålberg E V., Løseth S, Hødneø A & Lehmann-Horn F (2015). Painful cramps and giant myotonic discharges in a family with the Nav1.4-G1306A mutation. *Muscle and Nerve* **52,** 680–683.

Trip J, De Vries J, Drost G, Ginjaar HB, van Engelen BGMM & Faber CG (2009). Health status in non-dystrophic myotonias: close relation with pain and fatigue. *J Neurol* **256,** 939–947.

Trivedi JR (2022). Muscle Channelopathies. *Contin Lifelong Learn Neurol* **28,** 1778–1799.

Trivedi JR, Bundy B, Statland J, Salajegheh M, Rayan DR, Venance SL, Wang Y, Fialho D, Matthews E, Cleland J, Gorham N, Herbelin L, Cannon S, Amato A, Griggs RC, Hanna MG & Barohn RJ (2013). Non-dystrophic myotonia: Prospective study of objective and patient reported outcomes. *Brain* **136,** 2189–2200.

Villegas-Navarro A, Martinez-Morales M & Morales-Aguilera A (1986). Pharmacokinetics of anthracene-9-carboxylic acid, a potent myotonia-inducer. *Arch Int Pharmacodyn Ther* **280,** 5–21.

van Vliet J, Tieleman AA, Verrips A, Timmerman H, van Dongen RTM, van Engelen BGM & Wilder-Smith OHG (2018). Qualitative and Quantitative Aspects of Pain in Patients With Myotonic Dystrophy Type 2. *J Pain* **19,** 920–930.

Welsh MJ (1984). Anthracene-9-carboxylic acid inhibits an apical membrane, chloride conductance in canine tracheal epithelium. *J Membr Biol* **78,** 61–71.

Zhang J, George AL, Griggs RC, Fouad GT, Roberts J, Kwieciński H, Connolly AM & Ptáček LJ (1996). Mutations in the human skeletal muscle chloride channel gene (CLCN1) associated with dominant and recessive myotonia congenita. *Neurology* **47,** 993–998.

Figure Legends

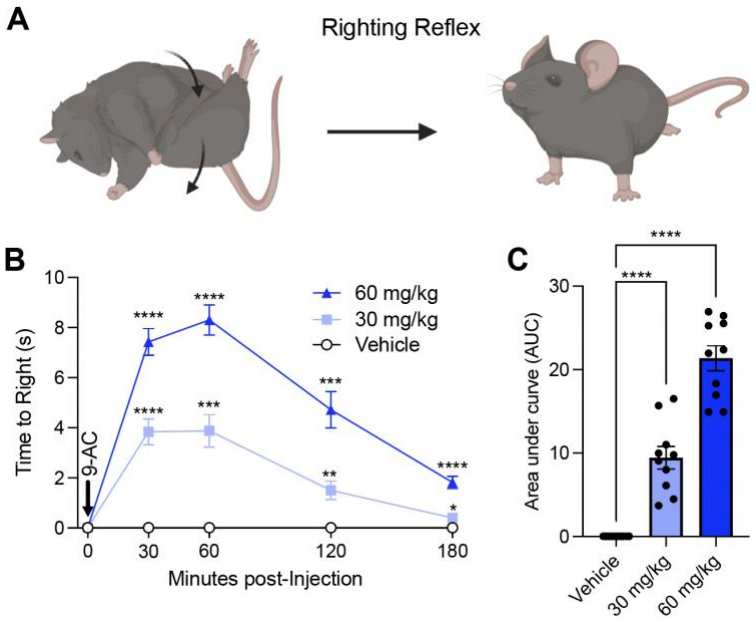

Figure 1. Anthracene-9-carboxylic acid (9-AC) produces *in vivo* myotonic behavior in mice.

(**A**) Schematic representation of the righting reflex.

(**B**) Intraperitoneal administration of 9-AC (30 mg/kg or 60 mg/kg) dose-dependently increases the time to righting reflex (n=10 mice/group). Two-way RM ANOVA. Holm-Sidak's post hoc test.

(**C**) Area under the curve (AUC) for righting reflex. (n=10 mice/group). One-way ANOVA. Holm-Sidak's post hoc test.

Data are shown as means ± SEM. *p < 0.05, **p<0.01, ***p<0.001, ****p<0.0001. Dots represent data points from individual animals.

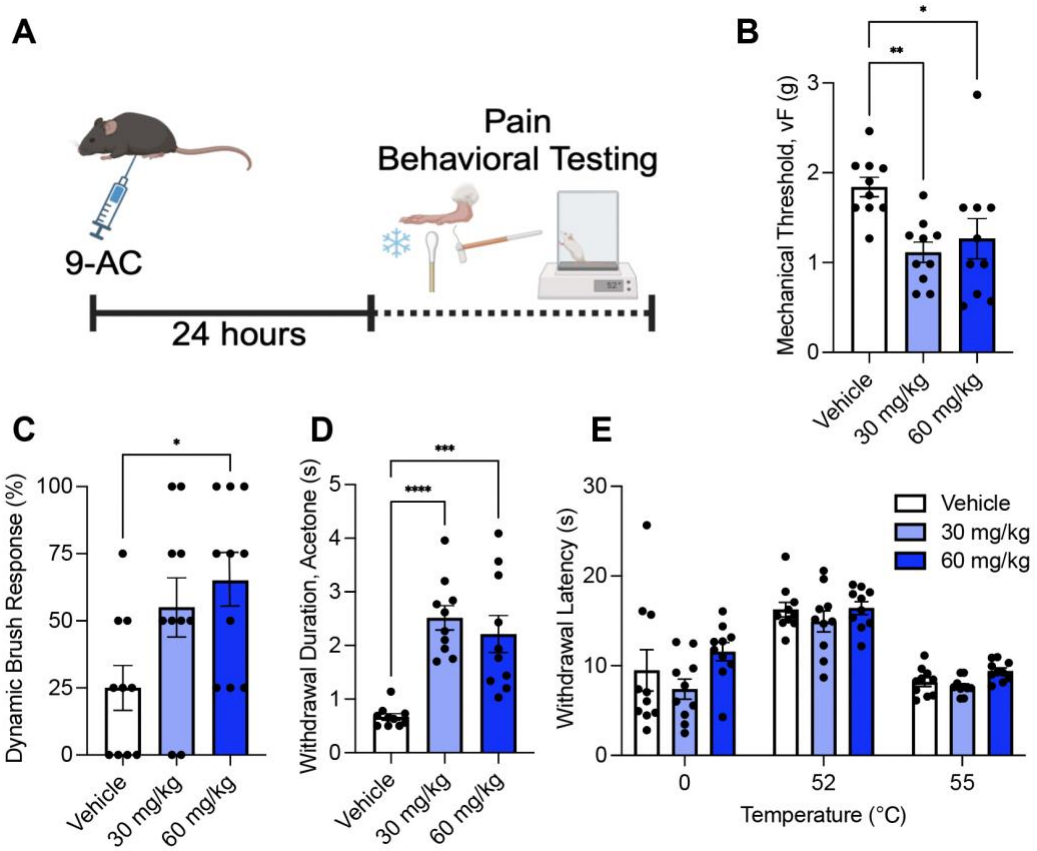

Figure 2. 9-AC induces chronic pain-like behavior in mice.

(**A**) Experimental timeline of 9-AC (30 mg/kg or 60 mg/kg, i.p.) administration and pain behavioral testing.

(**B-D**) 9-AC induces (**B**) static mechanical (von Frey, vF), (**C**) dynamic mechanical (brush responsiveness), (**D**) and cold (acetone droplet withdrawal) allodynia. (n=10 mice/group). One-way ANOVA. Holm-Sidak's post hoc test.

(**E**) Treatment with 9-AC did not elicit thermal hyperalgesia to noxious heat or cold stimuli (0, 52, and 55 °C hot/cold plate). (n=10 mice/group). Two-way RM ANOVA.

Data are shown as means ± SEM. *p < 0.05, **p<0.01, ***p<0.001, ****p<0.0001. Dots represent data points from individual animals.

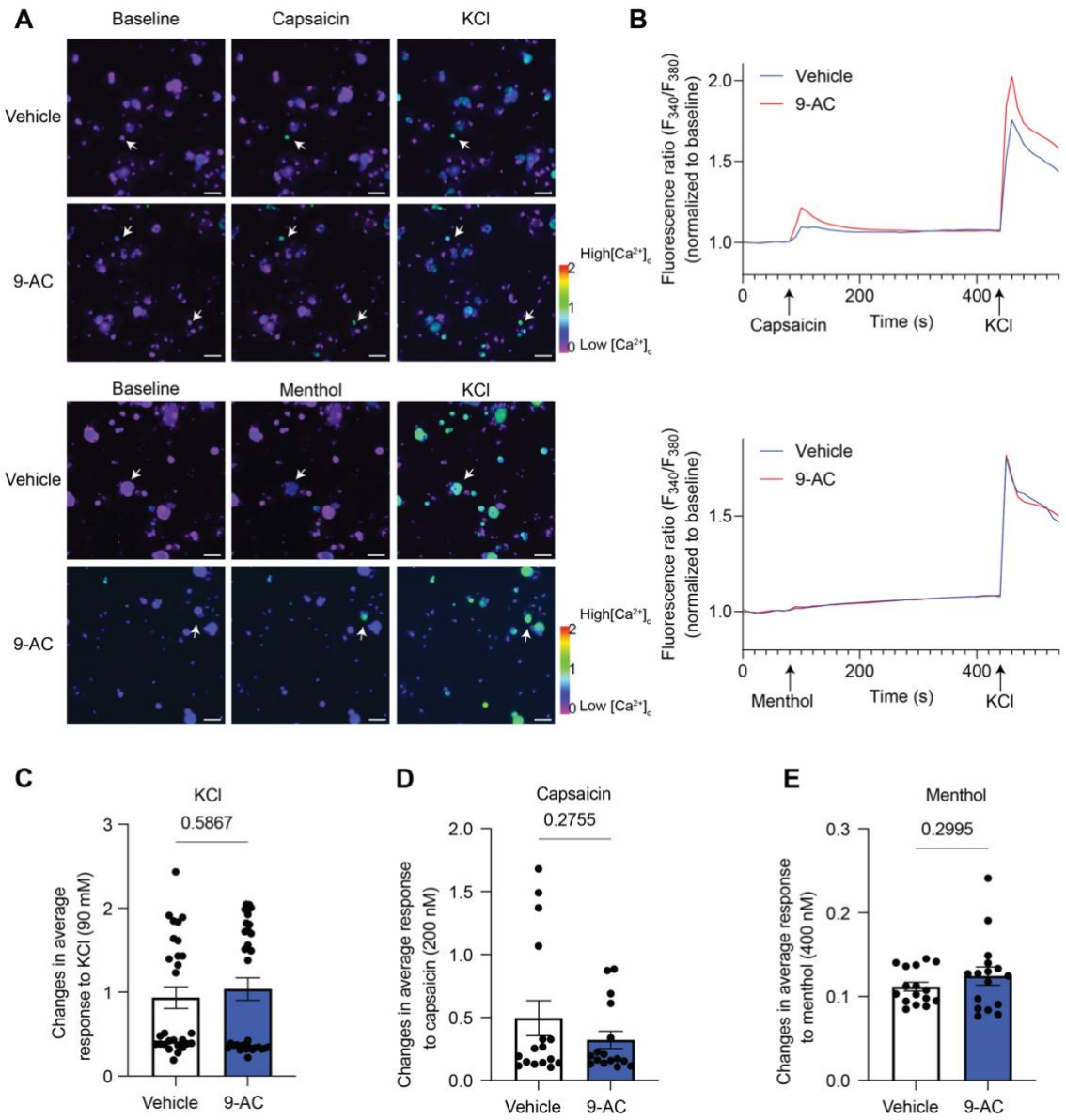

Figure 3. 9-AC treatment does not affect evoked Ca^{2+} influx in mouse dorsal root ganglion (DRG) sensory neurons.

(**A**) Representative images of DRG neuron responses to 90 mM potassium chloride (KCl), 200 nM capsaicin, and 400 nM menthol. Arrowhead shows a typical responding sensory neuron. Scale bar represents 25 μm.

(**B**) Average change in fluorescence ratio (F_{340}/F_{380}) over time after stimulation with capsaicin, KCl, and menthol.

(**C**) Bar graphs of average peak response to KCl in vehicle and 9-AC treated mice (n=28-31 coverslips from 4 animals/group, Vehicle=3549 total neurons and 9-AC=4073 total neurons). unpaired Student's two-tailed T test.

(**D**) Bar graphs of average peak response to capsaicin in vehicle and 9-AC treated mice (n=16 coverslips

from 4 animals/group, Vehicle=1054 total neurons and 9-AC=1069 total neurons). unpaired Student's two-tailed T test.

(**E**) Bar graphs of average peak response to menthol in vehicle and 9-AC treated mice (n=16 coverslips from 4 animals/group, Vehicle=747 total neurons and 9-AC= 993 total neurons). unpaired Students' two-tailed T test.

Data are shown as means ± SEM. p values are as indicated. Dots represent averages from all neurons on a treated coverslip.

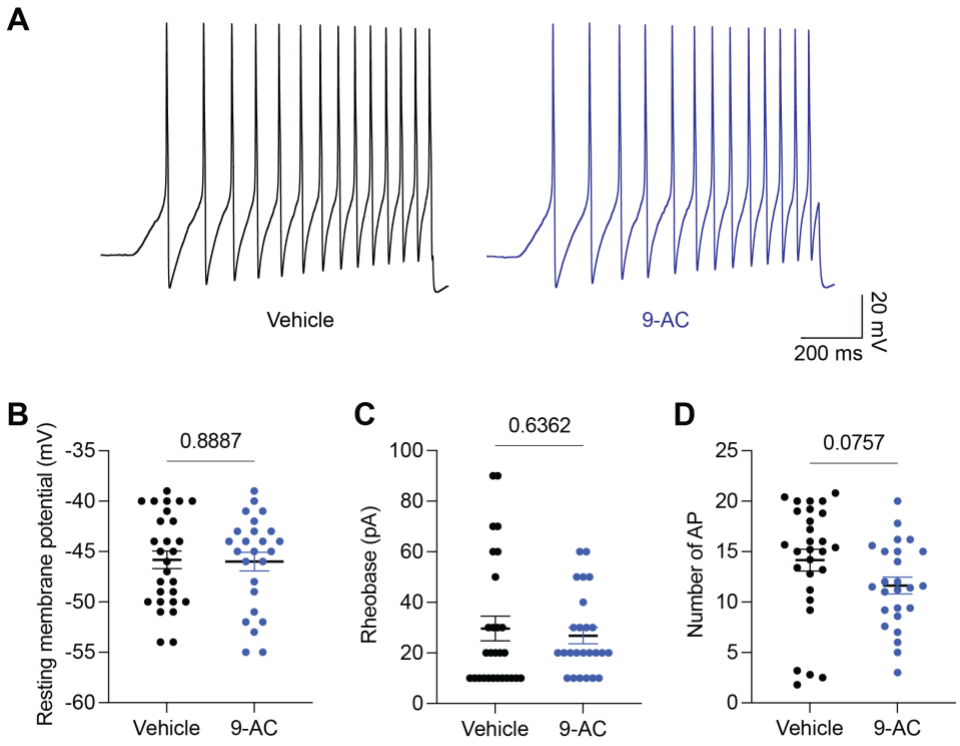

Figure 4. 9-AC treatment does not increase the excitability of DRG sensory neurons.

(**A**) Representative traces of the number of action potentials (AP) elicited in a sensory neuron from vehicle (left) and 9-AC (right) treated mice.

Using whole-cell current clamp electrophysiology we measured:

(**B**) Resting membrane potential (n=25-28 cells from 4 animals/group). unpaired Students' two-tailed T test.

(**C**) Rheobase (n=25-28 cells from 4 animals/group). unpaired Students' two-tailed T test.

(**D**) Number of AP (n=25-28 cells from 4 animals/group). unpaired Students' two-tailed T test.

Data are shown as means ± SEM. p values are as indicated. Dots represent individual neurons.

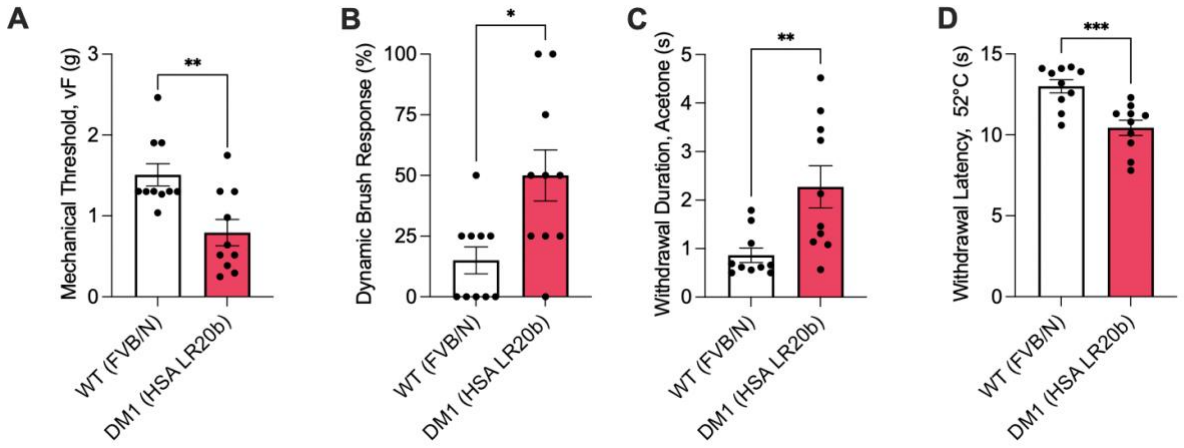

Figure 5. HSA LR20b myotonic dystrophy type 1 (DM1) mice exhibit nociplastic pain-like behavior. (**A-D**) In comparison to wildtype (WT) FVB/N background strain mice, HSA LR20b DM1 mice exhibit (**A**) static (von Frey, vF) and (**B**) dynamic (brush responsiveness) mechanical allodynia, (**C**) cold allodynia (acetone droplet withdrawal), and (**D**) thermal hyperalgesia (52 °C hot plate). (n=10 mice/group). unpaired Students' two-tailed T test.

Data are shown as means ± SEM. *$p < 0.05$, **$p<0.01$, ***$p<0.001$. Dots represent data points from individual animals.

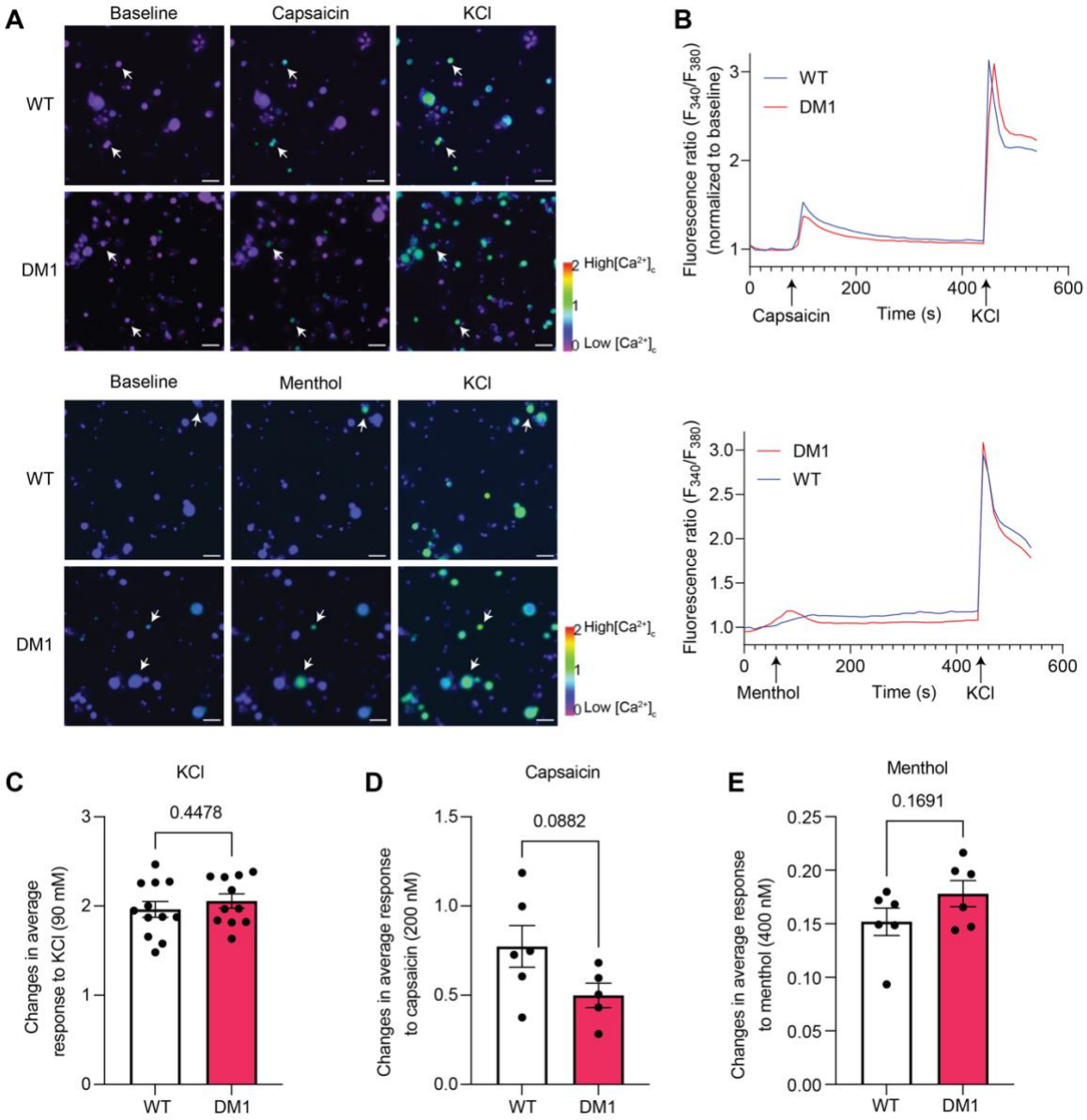

Figure 6. HSA LR20b DM1 mice do not exhibit changes in evoked Ca^{2+} influx in DRG sensory neurons.

(**A**) Representative images of DRG neuron responses in wildtype (WT) FVB/N and DM1 mice to 90 mM potassium chloride (KCl), 200 nM capsaicin, and 400 nM menthol. Arrowhead shows a typical responding sensory neuron. Scale bar represents 25 μm.

(**B**) Average change in fluorescence ratio (F_{340}/F_{380}) over time after stimulation with capsaicin, KCl, and menthol.

(**C**) Bar graphs of average peak response to KCl in WT and DM1 mice (n=12 coverslips from 2 animals/group, WT=1310 total neurons and DM1=2437 total neurons). unpaired Student's two-tailed T test.

(**D**) Bar graphs of average peak response to capsaicin in WT and DM1 mice (n=5-6 coverslips from 2

animals/group, WT=453 total neurons and DM1=450 total neurons). unpaired Student's two-tailed T test. (**E**) Bar graphs of average peak response to menthol in WT and DM1 mice (n=6 coverslips from 2 animals/group, WT=299 total neurons and DM1=614 total neurons). unpaired Students' two-tailed T test. Data are shown as means ± SEM. p values are as indicated. Dots represent averages from all neurons on a treated coverslip.